Title

Bidirectional low temperature district energy systems with agent-based control: Performance comparison and operation optimization

Authors

Bünning, Felix
Wetter, Michael
Fuchs, Marcus
et al.

Publication Date

2018

DOI

10.1016/j.apenergy.2017.10.072

Peer reviewed

Technical Report LBNL-2001090.
Cite as: Felix Bünning, Michael Wetter, Marcus Fuchs and Dirk Müller.
Bidirectional low temperature district energy systems with agent-based control: Performance comparison and operation optimization.
Applied Energy, Vol. 209, p. 502–515. 2017. DOI:10.1016/j.apenergy.2017.10.072

Bidirectional low temperature district energy systems with agent-based control: Performance comparison and operation optimization

Felix Bünning[1,2], Michael Wetter[1], Marcus Fuchs[2], and Dirk Müller[2]

[11]Lawrence Berkeley National Laboratory, Berkeley, USA
[12]RWTH Aachen University, E.ON Energy Research Center, Institute for Energy Efficient Buildings and Indoor Climate, Aachen, Germany

January 3, 2018

Abstract

Bidirectional low temperature networks are a novel concept that promises more efficient heating and cooling of buildings. Early research shows theoretical benefits in terms of exergy efficiency over other technologies. Pilot projects indicate that the concept delivers good performance if heating and cooling demands are diverse. However, the operation of these networks is not yet optimized and there is no quantification of the benefits over other technologies in various scenarios. Moreover, there is a lack of understanding of how to integrate and control multiple distributed heat and cold sources in such networks. Therefore, this paper develops a control concept based on a temperature set point optimization and agent-based control which allows the modular integration of an arbitrary number of sources and consumers. Afterwards, the concept is applied to two scenarios representing neighborhoods in San Francisco and Cologne with different heating and cooling demands and boundary conditions. The performance of the system is then compared to other state-of-the-art heating and cooling solutions using dynamic simulations with Modelica. The results show that bidirectional low temperature networks without optimization produce 26% less emissions in the San Francisco scenario and 63% in the Cologne scenario in comparison to the other heating and cooling solutions. Savings of energy costs are 46% and 27%, and reductions of primary energy consumption 52% and 72%, respectively. The presented operation optimization leads to electricity use reductions of 13% and 41% when compared to networks with free-floating temperature control and the results indicate further potential for improvement. The study demonstrates the advantage of low temperature networks in different situations and introduces a control concept that is extendable for real implementation.

1 Introduction

1.1 Background and motivation

District heating systems have been used for space heating and domestic hot tap water since the 1880s. Since then the efficiency of these systems has been improved continuously and four different generations of district heating systems can be distinguished, differing in heat carrier, temperature levels, circulation systems and substations [30].

With respect to the four different generations of

district heating systems, bidirectional low temperature networks (LTN) can be viewed as a fifth generation district heating and cooling system, as suggested by the European Commission [52]. They constitute an approach to further increase energy efficiency for heating and cooling of buildings by further lowering the fluid temperature in the networks to ambient temperature levels. The networks consist of two pipes. The warmer pipe has temperatures between 12°C and 20°C, while the cold pipe has 8°C to 16°C. Buildings equipped with heat pumps, chillers or direct cooling and individual circulation pumps are connected to both lines. In the case of a heating demand, the circulation pump of the building withdraws water from the warm line, uses it in a heat pump to reach temperatures suitable for space heating, and then discharges the cooled water to the cold line. In case of a cooling demand, the system works in the other direction. Depending on the heating and cooling demands of the connected buildings, the fluid flow in the network can change direction. The total difference between heating and cooling flows needs to be balanced by external sources, e.g. central heat pumps and chillers, solar thermal plants or seasonal storage facilities.

The concept is in the early stages of research and development. There is theoretical proof of the concept based on thermodynamic analysis [40]. Furthermore, there are at least eight demonstration projects (unidirectional and bidirectional) in operation or under construction (e.g [48, 27, 9]). Research regarding the optimal design in terms of diversity of cooling and heating loads has also been conducted lately [64].

Despite the previous efforts, there is a significant need for further research in multiple areas. It appears that no publications about control and operation optimization of LTN are available. There is proof that LTN are beneficial in terms of exergy efficiency, but the full potential has not been exploited yet. Moreover, there is a lack of understanding of how to integrate and coordinate multiple source networks in which individual so called "prosumers" can participate in heat and cold supply. Furthermore, there is only limited insight into the potential advantages a bidirectional LTN has over other technologies in different scenarios. To address these open questions is a crucial prerequisite for the future of sustainable heating and cooling systems through LTN technology.

Therefore, this study introduces, to the authors' knowledge, the first approach to operation optimization of low temperature networks. The approach consists of an optimization of the network temperature, which is the main influence on energy costs of such networks, and a control concept based on a market-based multi-agent system. With proper multi-agent control the electricity consumption of the heat pumps and chillers in the network can be lowered. Furthermore, the agent system allows the integration of multiple heat and cold sources and energy storages into the network, which makes it a practical approach for smart-grid-like decentral networks. The approach is verified with the help of dynamic simulations based on Modelica, for which the authors implemented the necessary models [60, 31] and the agent-based control system [2]. The case study examines two district scenarios, one of which is situated in the USA and one in Germany, and compares low temperature networks to other heating and cooling options. The results allow an insight into the behaviour of low temperature networks, present a proof of concept for the control approach and provide a quantification of energy cost savings through the use of low temperature networks instead of conventional heating and cooling technologies.

1.2 Previous work on low temperature networks

There is only a small number of peer-reviewed scientific work published in the field of bidirectional LTN. To give a complete overview of the topic, also reports on pilot projects by construction companies and other non-scientific sources are cited in the following.

One of the earlier examples of an LTN as described in this study was introduced in [10] as a plan to create a district heating and cooling system for a developing area in Visp, Switzerland. The unidirectional grid uses waste heat from a sewage of a chemical plant as a heat source and de-centralized heat pumps are used in the individual residential buildings to lift the temperatures sufficiently high to operate floor heating systems. [27] presents an evaluation of the system

installed in Visp. Completed in 2008, it has a total thermal capacity in heating of 3.6 MW and is competitive with other technologies in terms of cost of operation at a domestic fuel oil price below $0.9/lt.
In [48], an LTN for heating and cooling of parts of the campus of ETH Zürich is proposed. In order to reach the goals for a 2000-Watt-society [45], besides other measures, plans for a grid consisting of multiple ground heat storages, a geothermal field and de-central heat pumps are presented. Details on the progress can be found in [9].
Besides introducing the bidirectional concept, [46] makes several contributions to the topic of LTN: the author highlights the advantage of LTN in urban areas, where it is difficult to install heat pumps with individual ground or groundwater heat exchangers for residential buildings. Moreover, heat and cold demand should be of a similar size in the ideal case. The role for the operator of the system is to keep the temperatures at a sufficient level for cooling and heating and to balance the energy flows over the year in all storage facilities. It is further pointed out that LTN are modular and can be started as small projects that can be scaled up later on. A measure to further decrease operation costs could be the provision of grid services, as the used heat pumps constitute groups of high electrical capacities.
In [47], Sulzer examines the possibility of integrating solar thermal panels into LTN. The author states that integration of such systems is favourable in the case of seasonal heat storage as the demand for heat is higher in winter, but the production from solar thermal panels is high in summer. In [49], Sulzer et al. introduce different typologies of grids in terms of number of pipes between one and four. While the previously introduced bidirectional networks operate with two pipes at different temperature levels, third and fourth pipes with higher or lower temperatures are possible in order to use direct floor heating without a previous temperature lift via a heat pump, for example. Moreover, Sulzer now distinguishes between unidirectional and bidirectional grids in terms of mass flow and energy flow. A grid can be unidirectional in mass flow but bidirectional in terms of energy flow (e.g. in the case of Visp). Additionally, he presents several problems and unanswered questions related to the networks: So far, technological expertise is limited to a very small group of people. There are no standardized ways to calculate the cost of such a network for planners who were not involved in the pilot projects. Furthermore, the operation of LTN has not been optimized yet.
In [32], two different types of ownership for LTN are suggested. Bigger LTN could be owned by a grid operator, similarly to electrical grids or common district heating grids. Smaller grids could be owned and operated by the real estate owner. An example of a real-estate owned system in Chur, Switzerland, is given. A comparison between investment cost for a centralized heat pump system and an LTN is made and the LTN is found favourable. Furthermore, a comparison between yearly energy costs for the LTN in Chur and the local heating system installed before is made. A reduction of 62% of the annual energy costs could be observed.
Although focusing on heating grids with higher supply temperatures, Li et al. [29] point out that the development of future district heating grids will move away from hierarchical, fossil-based, large-scale structures towards future decentralized, multiple renewable and waste-heat-dominated small structures. Moreover, they postulate the idea that individual "prosumers" in the network who have the capacity to produce surplus heat from building installed solar collector, heat pump, micro-CHP and individual thermal storage, should be able to participate in the future grids. Pietra et al. [5] investigated the benefit of a grid connection for owners of solar thermal panels. The bidirectional grid operates as a virtual heat storage for the prosumer with the effect that the collectors can be operated throughout the whole summer instead of being stopped because of low heat demand during that period. Results show that the solar collector is able to supply more than 100% of the total yearly heat demand for an apartment when connected to the grid in comparison to 27% before, which leads to an operational cost reduction of 60%.
Gautschi [9] presents long-term experience with LTN. According to the building company, which built three LTN in the past, carbon emissions can be lowered by 70 to 80% and primary energy demand by 30 to 50% can be achieved. However, a reference technology

for these results is not given in the source. Furthermore, seasonal coefficients of performance from the system at ETH Zürich are reported with 7 for heating and 26.5 for space cooling. Two additional examples of LTN are presented. The system "Richti-Areal in Wallisellen" conditions offices and residential buildings with the help of 220 borehole heat exchangers with a depth of 220 m. The grid "Familienheim-Genossenschaft Zürich" uses wasteheat from a Swisscom data-center. Further heat producers are going to be added in the future.

Sulzer et al. [50] introduce a rapid-prototyping test bed, which allows to investigate the behaviour and control strategies of LTN. The system is designed as a hardware-in-the-loop test bed, which means that the integration of simulation-based methods is possible. First results of the test bed show that a ring-typology is favourable and could reduce pump energy by more than 50%. Furthermore, it is pointed out that a decentral pump design is more energy-efficient than a centralized one.

Vetterli et al. [57] show monitoring data from an LTN in operation in comparison to previous simulations of the same grid in the planning phase. The results show that the heating demand was underestimated and the cooling demand was overestimated, which leads to a decrease of temperature in the ground energy storage. Also the measured coefficient of performance (COP) is lower and circulation pump electricity consumption higher than predicted. The false predictions are ascribed to different user behaviour in terms of indoor temperature and ventilation (open windows) than expected. By adapting the model to the different user behaviour, reasonable accordance between measurement and simulation could be achieved.

In [16], the government of the canton St. Gallen in Switzerland presents financial measures to facilitate the building of LTN. The measures include the financial support for 5% of the building costs of the networks and a provision of $ 80 to 120 per MWh energy delivered during the first two years of operation. The government explicitly forbids the generation of heat with combined heat and power units.

Henchoz et al. [12] compared LTN to two different district heating and cooling concepts based on the use of latent heat with refrigerants (CO2 and R1234yf) as the heat carrying fluids. Simulation results show that none of the investigated grids has significant advantages in terms of energy efficiency over the other grids. It is also pointed out that no significant differences in terms of investment costs were present. The decision for one particular technology has therefore to be made based on soft characteristics, such as compactness or safety.

Summermatter et al. [51] introduce an LTN for a village in the Alps of Switzerland. Two possibilities, one based on the integration of solar thermal panels and one based on the integration of photovoltaic (PV) panels, are compared. The option featuring PV panels is found to be more cost efficient. The system uses the electricity from the PV panels to operate air-water heat pumps during the summer to heat up water. The heat is stored in a ground heat storage and can then be used with water-water heat pumps during the winter months. Moreover, the authors plan to offer grid services to the electricity grid in order to reduce costs. The grid will continuously be extended until the whole village is integrated.

Zach [63] presents a concept for an LTN in the district "Nordbahnhof" in Wien with 13,000 residents and 5,000 workplaces. The grid consists of one central LTN with a ground heat storage and five de-central grids connected to it. Photovoltaic thermal hybrid solar collectors are suggested as renewable heat and electricity sources after an annualized analysis of the system costs.

Zarin Pass et al. [64] explore the question of when and why bidirectional systems outperform their individual counterparts. The thermodynamic performance of bidirectional LTN is analyzed and a diversity criterion is developed to understand when it may be a more energy-efficient alternative to modern, high-efficiency individual-building systems. This criterion is then applied to standardized reference building hourly load profiles in three cities to look for promising building diversities. It is found that a bidirectional system has benefits when the ratio of heating to cooling loads on average is at least 1 to 5,7 or vice versa.

Research in modelling of LTN includes the following: Kräuchi et al. [22, 21] present a model in the object-oriented IDA-ICE simulation software. It uses

different objects for the components heat consumer, heat supplier, earth heat storage, pipes and pumps. Heat consumers and suppliers are modelled with the help of time series of demand and supply. Based on the desired temperature and the temperature of the grid, COPs for the heat pumps are calculated. There are models for the ground energy storage available that do not describe any temperature distribution in the ground, but act as a kind of fully mixed storage. The pipes are also modelled as fully mixed fluid volumes, but compute pressure losses. The pumps calculate mechanical and electrical power to compensate the pressure loss within the LTN. The model allows bidirectional flow. However, this feature is implemented by duplicating parts of the model for each direction of flow and activating or deactivating the relevant parts based on the current state of the system.
In [23] the above named model components are aggregated to a planned actual system. The results show good agreement with results from the planning phase of the grid. The authors therefore propose to use the models for the planning of LTN. Schluck et al. [40] use the described models in order to compare unidirectional and bidirectional grids. The results favour the bidirectional grid in terms of exergy efficiency and operating costs.
Prasanna et al. [35] present a model of parts of the Suurstoffi LTN [57] formulated as a mixed integer linear problem. The model is calibrated with monitoring data from parts of the grid. An optimization algorithm is then used to identify possible improvements of the system operation in order to reduce the carbon footprint of the network. Furthermore, possible scenarios regarding the extension of the system with components like additional photovoltaic or photovoltaic thermal hybrid solar collectors, battery storage and air-water heat pumps are simulated and compared.
The Modelica Buildings library [60] contains models to simulate LTN, including a water heat exchanger, central heat pumps and consumer substations. Other included models such as water storage tanks and solar thermal panels can also be used in an LTN district model. The models allow bidirectional flow.
Heissler et al. [11] present a modelling approach for the simulation of a low temperature district heating network with seasonal heat storage, collectors and buildings. The approach combines the simulation environments Dymola with the Modelica Buildings library and TRNSYS [33] with the help of the Building Controls Virtual Testbed [59]. The system model is a simple network with buildings with only heating demand, solar thermal panels and a water storage tank. A neighborhood in Munich is used as a case study.

1.3 Previous work on agent-based control of distributed energy systems

In this work a method to find an optimized temperature set point for a LTN is presented. In order to track the set point, feedback control is needed. Such a control algorithm needs to be able to orchestrate distributed heat and cold sources in an effective and stable way, in presence of distributed heat sources such as solar thermal roof panels. It should furthermore be flexible and expandable if additional buildings, storage or sources are added. Agent-based control is a concept which allows to control such complex systems by splitting the main control objective into smaller objectives which so-called agents try to fulfil by interacting with each other. Others used it to control electrical smart grids ([15], [20], [25], [62], [17], [19], [36], [37], [61] and [1]) and complex building systems ([14], [13], [42], [3] and [41]).

LTN are similar to electrical smart-grids and complex building energy systems. They feature distributed sources for heat and cold as well as distributed consumers of heat and cold. A control system for an LTN needs to maintain the temperature in both temperature lines within a usable range for heat pumps and chillers. This needs to be done by balancing supply and demand. The principle is analogous to the control mechanisms implemented in electrical grids, where supply and demand need to be coordinated in order to keep the voltage within a range. Similar analogies can be found in complex building energy systems, such as the building presented in [8]. As agent-based control has been shown to be an efficient way to implement control for smart-grids

and complex building energy systems, and as LTN provide control problems which are similar to those found in smart-grids and complex building energy systems, agent-based control is used in the course of this work to control the LTN.

2 Methodology

We will now describe the methodology used in our study.

In order to optimize the operation of LTN, we used a cascading control as shown in Fig. 1. It consists of an optimization of the temperature set point profile for the network and a following sequence of control steps, including agent-based control, to maintain the optimized temperature set point in the network with multiple heat and cold sources. The optimization and control steps will be presented in the following section.

2.1 Temperature set point optimization

Fig. 2 and Fig. 3 show the Carnot COP of a heat pump and a chiller, respectively, as a function of the temperature of the fluid in the pipe. A constant $\triangle T$ of 2K between water and refrigerant is assumed in condensers and evaporators. As for the efficiency of heat pumps, high pipe temperatures are favourable whereas for chillers low temperatures are favourable, there is a potential for optimization to find the optimum temperature. However, in previous research, a free floating temperature approach was usually used, in which the warm line temperature is kept between a lower and a higher limit. Between these limits it changes depending on the heating and cooling demands of the consumers. Finding a suitable set point through numeric optimization is our first step.

The system is optimized for a cost function that represents a performance metric. As the cold line temperature depends on the warm line temperature, the optimization only searches for a set point for the warm line. The cost function can for example be primary energy consumption, electricity consumption or carbon emissions. As the only costs are generated by the heat pumps and chillers, these cost functions are proportional to each other if constant emission and primary energy factors are assumed. Therefore, the outcome of the optimization is independent of this selection. For example, the cost function for electricity consumption follows

$$Cost = \int_0^\tau \left(P_{\mathrm{chi}} + P_{\mathrm{hp}}\right) dt, \tag{1}$$

where $Cost$ is the value of the cost function, P_{chi} is the electrical power of all chillers and P_{hp} is the electrical power of all heat pumps.

In order to maintain comparability with the previously used free floating approach, the set point is constraint by $12°C$ and $20°C$.

The optimization problem was formulated as

$$\begin{aligned} \underset{\{a,b,c\}\in\Re}{\text{minimize}} \quad & f(T_{\mathrm{set,wl}}), \\ \text{subject to} \quad & T_{\mathrm{set,wl}} = a + b\left(\frac{\dot{Q}_h}{\dot{Q}_{h,max}}\right)^n + c\left(\frac{\dot{Q}_c}{\dot{Q}_{c,max}}\right)^n, \\ & T_{\mathrm{set,wl}} \in [12°C, 20°C], \end{aligned} \tag{2}$$

where $T_{\mathrm{set,wl}}$ is the set point for the warm line and $n \geq 0$ is a constant. For $n = 0$, $T_{set,wl}$ is a constant. For $n = 1$, the set point is linear in the load, unless the constraint $T_{\mathrm{set,wl}} \in [12°C, 20°C]$ is active. As we will see below, it turns out that a constant set point suffices, and hence we will below only compare the cases for $n \in \{0, 1, 4\}$, with $n = 4$ selected to show the effect of a large exponent. The evaluation of the cost function $f\colon \Re \to \Re$ involves a simulation of a Modelica model which is a simplified model of the ones used for the case study. It uses hourly load data for heating and cooling loads for a district and models the electricity consumption of heat pumps and chillers for individual building types with the help of a Carnot approach. The heat pumps use an ideal water source at $T_{set,wl}$ on the evaporator side, while the chillers use an ideal water source of $T_{set,wl} - 4K$ on the condenser side. A different model is used for the optimization than in the case study. In the optimization model the pipe network and the electricity consumption of the circulation pumps is not modelled to increase optimization speed.

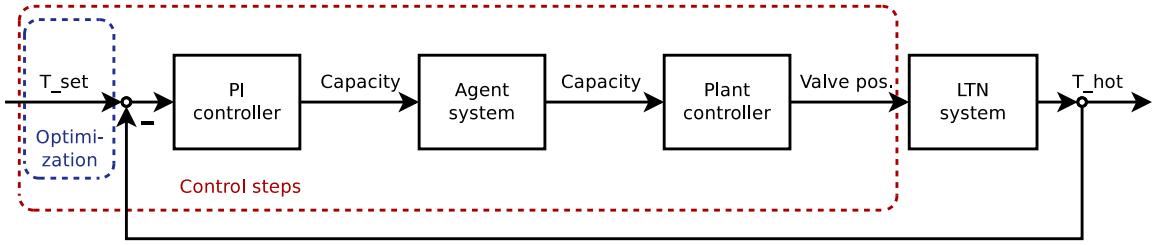

Figure 1: Optimization and control scheme for low temperature networks

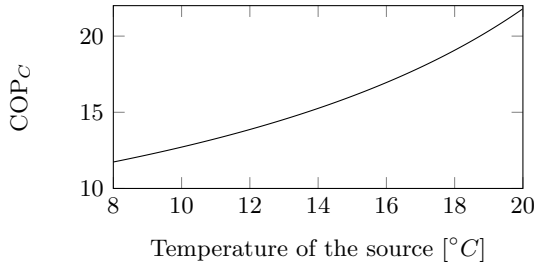

Figure 2: Carnot Coefficient of Performance of a heat pump with $T_{hea} = 30^\circ C$ with $\triangle T = 2K$ in heat exchangers

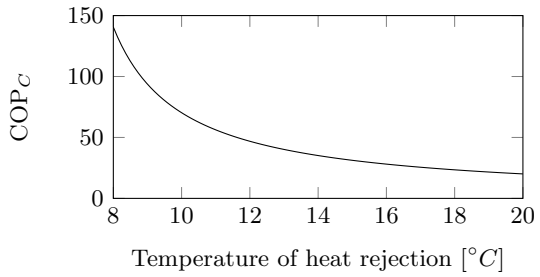

Figure 3: Carnot Coefficient of Performance of a chiller with $T_{coo} = 10^\circ C$ with $\triangle T = 2K$ in heat exchangers

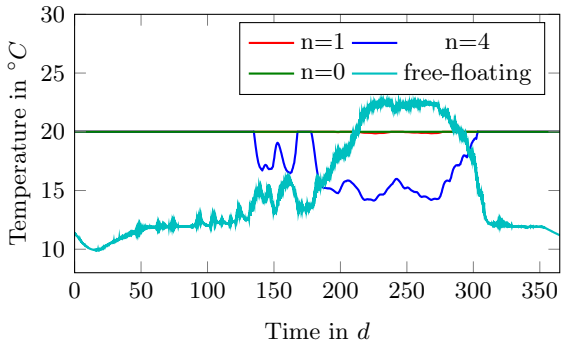

Figure 4: Temperature set points of the warm line after optimization

The optimization was done in Python 2.7. To automate the optimization, the standard Dymola-Python interface, which is provided with Dymola, was used. The simplex method Nelder-Mead with default parameters and tol = 1E-6 from the Python SciPy package was used to solve the optimization problem.

Fig. 4 shows the results for $T_{set,wl}$ of the optimization for the San Francisco case (see section 3). In the free floating case, one can see that the temperature is lowest during winter, as heating dominates cooling, which results in a temperature drop of the whole network. The highest temperatures are reached in late summer when cooling is high. Consequently, the temperatures in the network rise. Contrasting this behaviour to the COP of heat pumps and chillers, it becomes clear that a free floating temperature causes the grid to establish temperatures that are opposite of the ideal case. The grid is warm when it should be cold and is cold when it should be warm.

It can be noticed that all optimized results have a higher average temperature than the free floating case. Besides a slightly lower temperature in the late summer days, the linear approach does not differ much from the constant approach. For n=4, the temperature during summer is lowered by 6 K. This is expected because the cooling load is higher in summer and lower temperatures are favourable for the performance of chillers.

However, the cost function values are all within 1%. Hence, n has little effect on the performance. Thus,

whether the line temperature during summer is at 20 °C or at 14 °C has little impact on performance. However, the free floating case shows a 15% higher electricity consumption.

The surprising result can by explained by further examination of the network performance at different load ratios. Neglecting the power consumption of the pumps, assuming that non-balanced heat in the distribution network can be made up with renewable energy or storage that shifts loads, and assuming a constant Carnot efficiency η, the normalized electricity consumption is

$$p_{el} = \frac{1}{\eta}\left(\frac{\dot{q}_h}{COP_h} + \frac{\dot{q}_c}{COP_c}\right), \tag{3}$$

where $\dot{q}_h$ is the normalized heating load, $\dot{q}_c$ is the normalized cooling load, COP_h is the Carnot coefficient of performance for heating and COP_c is the Carnot coefficient of performance for cooling. Using $COP_h = T_h/(T_h - T_c)$ and $COP_c = T_c/(T_h - T_c)$, where T_h and T_c are the refrigerant temperatures in the condenser and evaporator, we can write (3) as

$$p_{el} = \frac{1}{\eta}\left(\dot{q}_h \frac{T_h - T_c}{T_h} + \dot{q}_c \frac{T_h - T_c}{T_c}\right). \tag{4}$$

Let T_{wl} and T_{cl} be the water temperatures in the warm and cold pipe, let T_{hea} be the space heating supply temperature and T_{coo} be the space cooling supply temperature,let $\Delta T_l \triangleq T_{wl} - T_{cl}$ and let $\Delta T_r > 0$ be the temperature difference between water and refrigerant. Then, we can write (4) as

$$p_{el} = \frac{1}{\eta}(\dot{q}_h \frac{(T_{hea} + \Delta T_r) - (T_{wl} - \Delta T_r)}{T_{hea} + \Delta T_r} + \dot{q}_c \frac{(T_{wl} - \Delta T_l + \Delta T_r) - (T_{coo} - \Delta T_r)}{T_{coo} - \Delta T_r}). \tag{5}$$

Assuming $\eta = 1$, $T_{hea} = 30$ °C, $T_{coo} = 10$ °C, $\Delta T_r = 2$ K in all heat exchangers and $\Delta T_l = 4$ K , the normalized electrical consumption is as shown in Fig. 5. It turns out that $p_{el,network}$ is linear in the warm line temperature.

The plot shows that electricity consumption for higher heating ratios (red) is generally higher than for higher cooling ratios (blue). This can be explained by the generally higher coefficient of performance of chillers compared to heat pumps. Furthermore, it can be seen that the performance curve of the network at equal heating and cooling load is nearly flat, which explains the results of the optimization. As heating and cooling loads are of similar magnitude in the summer months for the San Francisco scenario, low temperature set points during summer perform equally well as high ones. For this case, it can be stated that a well-chosen temperature set point during winter with high heating loads is more important to the network performance than the set point during summer.

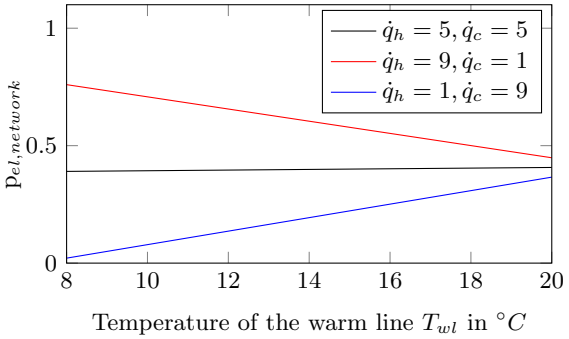

Figure 5: Relative electricity consumption for different heating to cooling ratios

As all set point optimizations showed similar cost function values, only the most simple one, the constant temperature approach, was chosen for the case studies. For a transfer to a real system, this approach is more suitable than the others as no load data need to be measured. The same approach was chosen for the Cologne case, as the optimization showed similar results.

2.2 Control steps with agent-based control

In the above section, a method to find an optimized temperature set point for the network was presented. In order to track the set point, agent-based control is used.

Fig. 6 shows the LTN equipped with the agent-based control system. The two lines with warm and

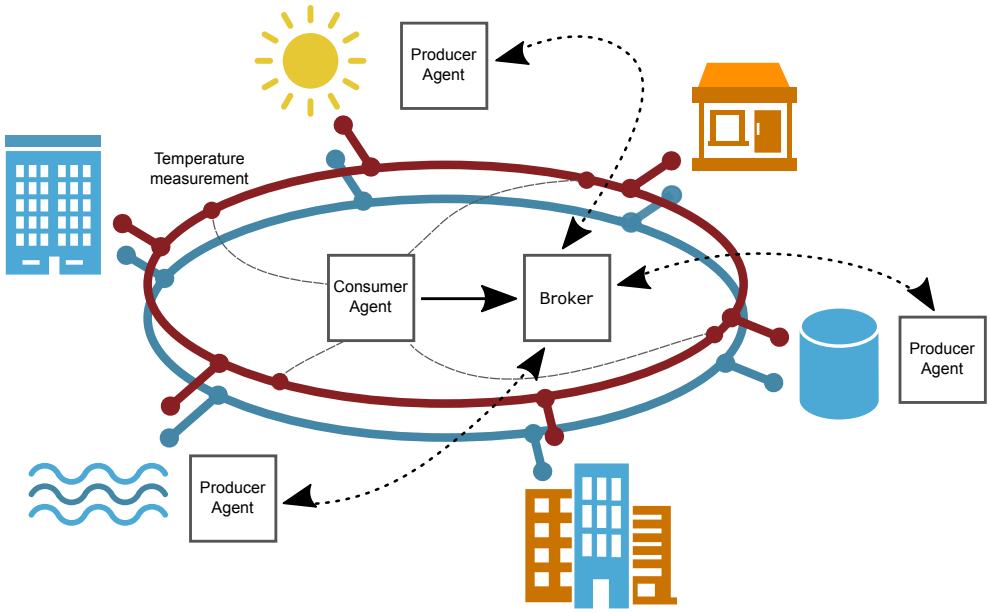

Figure 6: Bidirectional low temperature network with agent-based control

cold temperature level are represented by the red and blue ellipses. The network has heat and cold consumers represented by the orange and light blue buildings connected to the network. Besides these consumers, also three producers are connected to the network: a solar thermal panel, a water heat exchanger and a water storage tank. It should be mentioned that consumers generally are also producers in a bidirectional LTN, for example, a heat pump consumes heat while producing cold. However, we mean by producer a facility whose main task is to maintain the right network temperature, and by consumer a facility whose main task is to heat or cool buildings.

The network is controlled as follows. The temperature of the network is measured at multiple points that are evenly spread along the warm circular pipe (in this case four points) and an average temperature is computed. This temperature is compared to the temperature set point $T_{\mathrm{set,wl}}$ after a low pass filter. A PI controller with anti-windup converts the difference between the current average warm line temperature of the network and $T_{\mathrm{set,wl}}$ into a demand for heating or cooling. The consumer agent sends its capacity demand to the broker. The broker then proceeds to call for a proposal from each producer agent in the system. With the help of a cost function, each producer agent computes a proposal for the requested capacity adjustment. If a producer is not able to make the adjustment, it can refuse the call for proposal by the broker. When the broker has collected the proposals (and refusals) of all producer agents, the proposals are compared and the most cost-efficient combination is selected. Notifications of accepted and refused offers are sent to the producer agents. The producer agents then adjust the capacity of the producer they represent.

In contrast to a building energy system, the renewable producers in this example of an LTN do not produce real costs during their operation because they produce heat or cold close to zero marginal cost. Therefore, a virtual cost function is necessary as a measure of cost. The cost function is based on the temperature difference of the water that the producer can supply and the current network temperature. The cost function for a heat supplier is

$$C = Cap\,(T_{set,wl} - T_{source}), \tag{6}$$

where C is cost, Cap is the capacity of the source, $T_{set,wl}$ is the set point temperature of the hot line and T_{source} is the supply temperature of the source.

Similarly, for cold suppliers, the cost is

$$C = Cap\,(T_{source} - T_{set,cl}), \tag{7}$$

where $T_{set,cl} = T_{set,wl} - 4K$ is the set point of the cold line. In (6) and (7), the temperature gives lower cost the closer a source is to the set point. For example, if $T_{set,wl} = 20°C$ and heat sources at $18°C$ and $19°C$ are available, the source at $19°C$ is chosen in order to optimize the network performance.

In the last step of the control sequence, the capacity requested from a producer agent needs to be translated into an enthalpy change in the network fluid. In the case of low exergy sources such as water heat exchangers and seasonal storage facilities, this is done with a P controller and a valve which regulates the resulting mass flow induced by the individual consumer pumps. In the case of a high exergy source, such as solar thermal panel, a pump which induces additional mass flow instead of a valve is used in order to obtain better network penetration and as a result more even network temperatures. In both cases, the absolute value of the requested capacity is used as the set point for the P controller and the absolute value of the enthalpy difference upstream and downstream of the source as the measurement input. Absolute values are necessary in order to handle the possible change of flow direction in the source, and to keep the control stable.

3 Case study

To quantify the benefits of LTN and to verify the presented control strategy, different scenarios were analyzed using Modelica. Two different example districts,the Shipyard neighborhood in San Francisco, USA, and the Rheinauhafen district in Cologne, Germany, were selected. The scenarios differ from each other in terms of type and amount of buildings, insulations standards, and climate leading to different heating and cooling loads. For both scenarios, a comparison of the following technologies was made:

- Conventional gas-fired district heating and stand-alone chillers
- Stand-alone heat pumps and chillers
- Unidirectional LTN with free floating temperatures
- Bidirectional LTN with free floating temperatures
- Bidirectional LTN with agent-based control and multiple sources

3.1 Load data and boundary conditions

In order to model heating and cooling loads for the San Francisco scenario, information on the distribution of buildings in the neighborhood was gathered from [28]. With the help of the information on the type of buildings and the area occupied by these buildings, load profiles were created using Department of Energy reference models [53]. Because early simulations indicated that the given number and types of buildings would lead to an unbalanced network, not all residential buildings were connected to the network. The resulting floor area consists of 72% for offices, 16% for housing and 12% for retail. Fig. 7 shows the integrated heating and cooling loads for the neighborhood per m^2 floor area. One can see that the heating load is bigger than the cooling load during winter, but the system is well balanced during the summer months. The annual diversity index calculated after [64] is $div_{annual} = 0.70$, which is a value that indicates that a bidirectional LTN should perform well in this scenario. Weather data for the simulation was taken from TMY3 San Francisco International Airport. Water temperatures for the ocean heat exchanger were taken from [55] for the nearby city of Alameda, which is 8 km north-east of the neighborhood. The temperatures are shown in Fig. 8. Tab. 4 shows the main parameters of the San Francisco location.

For the Cologne scenario, information on the distribution of building types was obtained from [39]. The total floor area consists of 60% office space and 40%

housing. To generate load curves, the Python package TEASER (Tool for Energy Analysis and Simulation for Efficient Retrofit) [38] and Modelica simulations were used. TEASER allows the creation of archetype building model records for a low-order building model of the AixLib [31] library and Buildings [60] library . Fig. 9 shows the integrated loads per m^2 floor area for the Cologne scenario. One can see that there is only a limited amount of overlapping between heating and cooling loads. Additionally, in the periods in which both types of loads occur, they do not occur during the same hours (heating at night, cooling during the day). This leads to an annual diversity index of $div_{annual} = 0.04$. As there is no data on Rhine water temperatures available for the city of Cologne, data from the Düsseldorf-Flehe station from 2015 was used instead [26], which is 40km away from Cologne. TRY2012 data from Aachen ($63km$ from Cologne) was used to simulate the weather. Fig. 10 shows water and ambient air temperatures. Tab. 5 shows the main parameters of the Cologne location.

Operating temperatures are 30 °C for supply and 25 °C for return in case of space heating, 16 °C for supply and 20 °C for return in case of space cooling and 60 °C for supply in case of domestic hot tap water in all models and both locations.

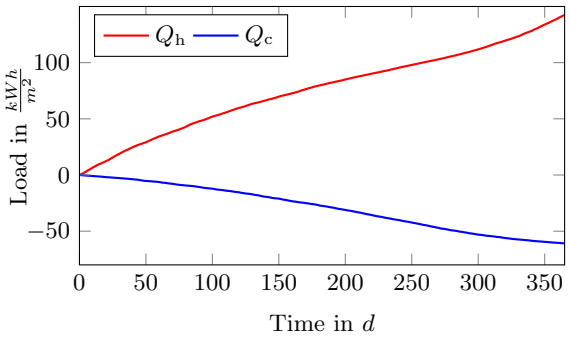

Figure 7: Heating and cooling load in San Francisco scenario

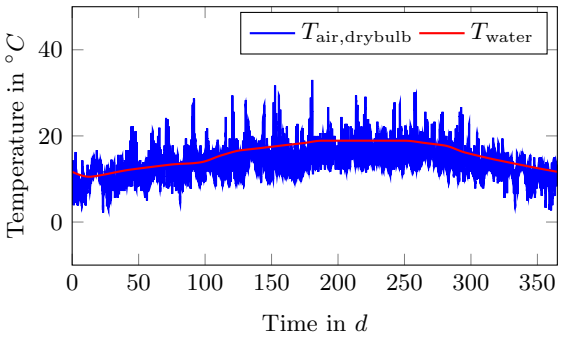

Figure 8: Air and water temperatures in San Francisco scenario

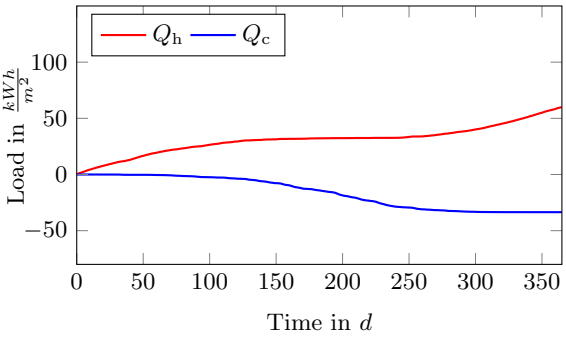

Figure 9: Heating and cooling load in Cologne scenario

3.2 Models for the investigated technologies

For each heating and cooling technology, a dynamic Modelica model was created. All thermal and hydraulic models were built and aggregated using the Modelica Buildings Library (branch issue653_carnot_dt, commit add1439) [60] and the AixLib library (master branch, commit 4b7047c) [31]. The agent-based control elements were realized with the Modelica HVACAgentBasedControl library (also accessible through AixLib) [2]. The aggregated system models can be requested from the authors. Each model will be described in the following section.

3.2.1 LTN with agent-based control and multiple sources

Fig. 11 shows an overview of the hydraulic set up and the control signals of the model for the bidirectional

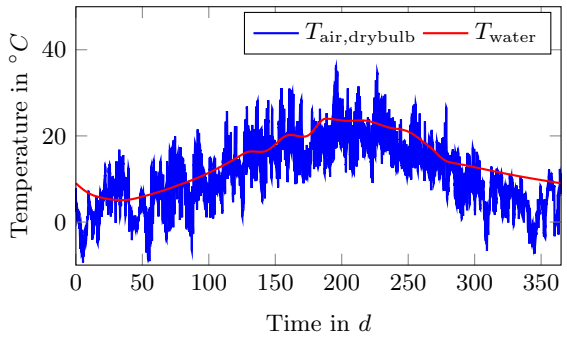

Figure 10: Air and water temperatures in Cologne scenario

LTN with agent-based control. The schematics shows as an example one consumer with the evaporator of a heat pump and the condenser of a chiller. The actual model has more than one consumer and separate heat pumps for space heating and domestic hot tap water. The heat and cold consumers were modelled as substations based on hourly load data for heating and cooling demands. Heat pumps and chillers use a Carnot-efficiency-based approach with $\eta = 0.45$ and a temperature difference in the heat exchangers dependent on the load ratio with $\triangle T_{r,max} = 2K$ in order to determine their electricity consumption. The total substation electricity consumption includes the heat pumps, chillers and circulation pumps. Also shown are the three supply plants, consisting of water heat-exchanger that is connected to a river, lake or ocean, storage tank and solar thermal plant. The two latter ones are equipped with producer agents, which control the valve and the pump. The valve of the water heat exchanger acts as a bypass for the storage tank. The hydraulic network is modelled with pipe models that account for pressure losses based on flow-rate dependent flow friction and thermal losses or gains. (For more details on the models please refer to [58] and the documentation within the open source Modelica Buildings Library [60]). The total length of the network in San Francisco and Cologne are 8 km and the pipes are sized to accommodate the nominal mass flow at a flow velocity of 1.5 $\frac{m}{s}$. The pipes are insulated with a 20 cm layer with a heat transfer coefficient of 0.04 $\frac{\text{W}}{\text{mK}}$. For the boundary condition of the thermal losses, a undisturbed ground temperature model which accounts for seasonal change of the ground temperature is used [24]. The pipe network is divided in one hundred control volumes, each with a fully mixed temperature.

Important parameters of the system are given in Tab. 6 for San Francisco and in Tab. 7 for Cologne. Apart from that, the models for San Francisco and Cologne only differ in heating and cooling demands, weather and water temperatures for the water heat exchangers, as described in the previous section.

In order to assess the network performance, the electricity consumption of all relevant appliances in the system is

$$E_{\text{prim}} = \int_0^\tau PEF_{\text{el}} \left(P_{\text{pumps}} + P_{\text{chi}} + P_{\text{hp}}\right) dt, \quad (8)$$

where E_{prim} is the primary energy consumption, PEF_{el} is the primary energy factor for electricity, P_{pumps} is the electrical power of all circulation pumps, P_{chi} is the electrical power of all chillers and P_{hp} is the electrical power of all heat pumps.

3.2.2 Bidirectional LTN with free-floating temperatures

Fig. 12 (A) shows the hydraulic system for the bidirectional LTN with free floating temperatures. The only heat and cold source is a water heat exchanger. The water heat exchanger is controlled to keep the warm line temperature between 12°C and 20°C and the cold line temperature between 8°C and 16°C. The pipe network and substations are identical to the LTN with agent-based control and multiple sources.

3.2.3 Unidirectional LTN with free-floating temperatures

Fig. 12 (B) shows the hydraulic system for the unidirectional LTN with free floating temperatures. Again, the only heat and cold source is a water heat exchanger. It is controlled to keep the water temperature within the same limits as in the bidirectional LTN. In the unidirectional LTN, heat pumps and chillers draw water from the same supply line and discharge to the same return line. Therefore,

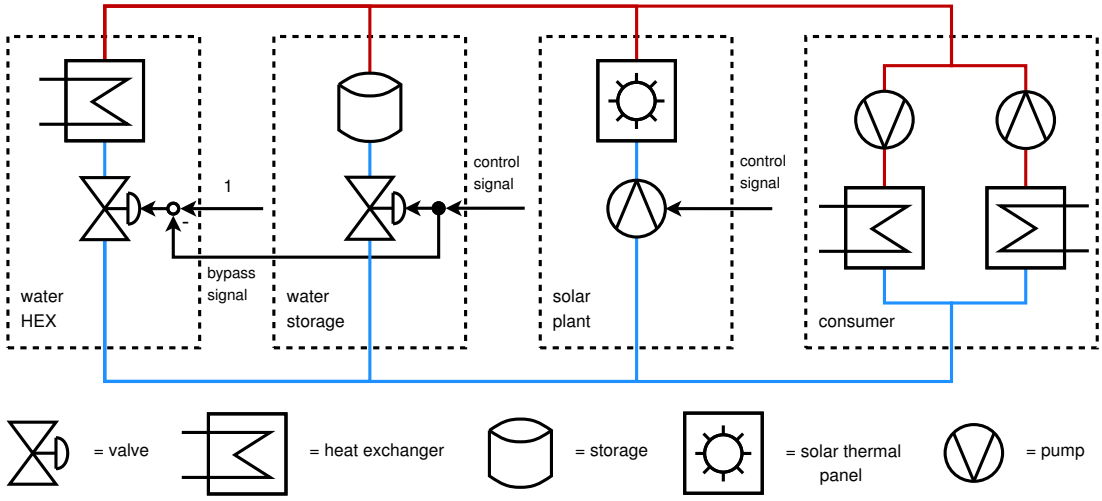

Figure 11: Bidirectional LTN with multiple sources model schematic

the pump of the chillers in the substations is turned around. The pipe network has the same length, diameter and insulation as in the bidirectional LTN. Also the efficiency of the heat pumps and chillers in the substations is computed with the same approach as in the bidirectional systems.

3.2.4 District heating with stand-alone cooling

Fig. 13 (A) shows the hydraulic scheme for the district heating with stand-alone cooling on the left-hand side and the solution with stand-alone heating and cooling on the right-hand side. The district heating system uses a central natural gas heater with a thermal efficiency of 0.95. The heater is controlled to supply a constant water temperature of 90 °C. Individual pumps at the consumer substations control the mass-flow in order to reach return temperatures of 60 °C. The network is also dimensioned to accommodate the nominal mass-flow rate at a velocity of 1.5 $\frac{m}{s}$. This leads to smaller diameters (26 cm) than in the LTN case (71 cm), as the temperature spread between supply and return is much bigger. Furthermore, an insulation layer of 40 cm with a heat transfer coefficient of 0.035 $\frac{\mathrm{W}}{\mathrm{mK}}$ (compare [43]) is used in order to reduce thermal losses. In the substations, a simple heat exchanger with 100% efficiency is used instead of the heat pump for space heating and domestic hot tap water in the substations. To meet the cooling demand, a chiller that is connected to the ambient air is used. The main parameters of the system are given in Tab. 8.

To assess the performance of the conventional district heating scenario, the primary energy is

$$E_{\mathrm{prim}} = \int_0^{\tau} [PEF_{\mathrm{gas}}\, W_{\mathrm{gas}} + PEF_{\mathrm{el}}\, (P_{\mathrm{pumps}} + P_{\mathrm{chi}})]dt, \tag{9}$$

where PEF_{gas} is the primary energy factor for natural gas and W_{gas} is the chemical work of the natural gas.

3.2.5 Stand-alone solution

Fig. 13 (B) shows the stand-alone solution. The substations use heat pumps and chillers which are both connected to the ambient air. There is no piping network in this scenario. Parameters of the heat pumps and chillers are identical to the LTN cases. The performance evaluation for the pure stand-alone case follows (8).

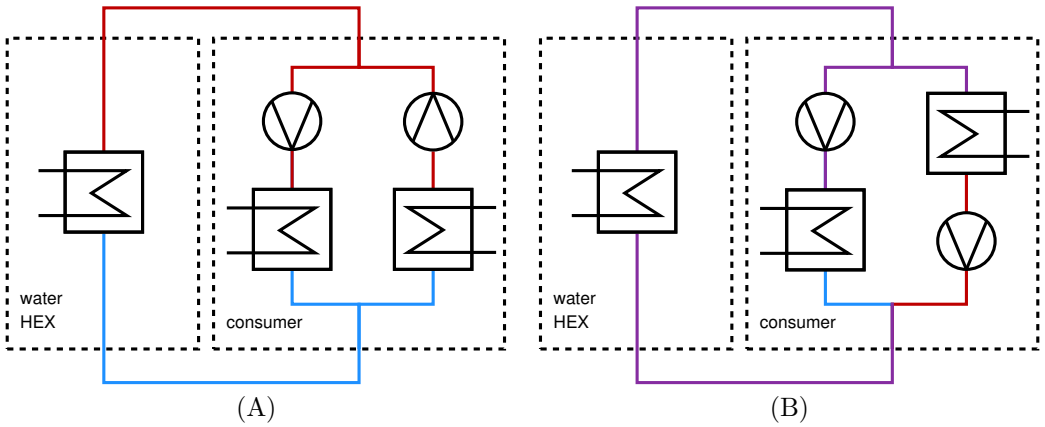

Figure 12: (A): bidirectional LTN with water heat exchanger schematic, (B): unidirectional LTN with water heat exchanger schematic

4 Results and discussion

4.1 Primary energy usage, emissions and energy costs

Fig. 14 (A) and Fig. 14 (B) show the relative primary energy consumption, normalized by the maximum primary energy consumption for the case studies San Francisco and Cologne respectively. Primary energy factors for electricity and natural gas, taken from [4] and [6], were used as stated in Tab. 1.

Table 1: Primary energy factors used in simulation

Energy carrier	San Francisco	Cologne
Natural gas	1.09	1.10
Electricity	2.89	1.80

Both scenarios show that solutions with heat pumps generally perform better than the district heating solution. In the Cologne scenario the difference between district heating and stand-alone solution is of higher magnitude than in the San Francisco scenario because the primary energy factor for electricity in Germany is lower than for the western USA. However, the difference is not proportional to the difference in primary energy factors, as the climate in San Francisco is milder than the one in Cologne, which leads to better heat pump and chiller performance. In comparison to the stand-alone solution, a bidirectional LTN with free-floating temperature control decreases the primary energy consumption by 9% in San Francisco and 13.5% in Cologne. The selection of a bidirectional network instead of a unidirectional network leads to an improvement of 5% in San Francisco but only 1.5% in Cologne. This can be explained by the shape of the heat and cold demands (compare Fig. 7 and Fig. 9) and the exergy destruction of mixing fluid streams of different temperatures. In the case of San Francisco, there is a higher occurrence of heat and cold demands at the same time than in the Cologne case, where heat is mainly used during winter and cold during summer. The advantage of bidirectional networks in terms of exergy efficiency is the avoidance of mixing the warm return streams from the chillers and the cold return streams from the heat pumps in one common return line, as discussed in [40]. In the case where heat and cold demands are separated, the exergy destruction in the mixing nodes does no longer take place. Between the cases bidirectional LTN with free-floating temperature and bidirectional LTN with agent-based control, the primary energy consumption could be further lowered by 13% in the San Francisco scenario and 41% in the Cologne scenario. The higher improvement in the Cologne case can again be explained by the different boundary conditions. Both bidirectional models use water heat exchangers. In the case of San Francisco, the heat exchanger exchanges heat with

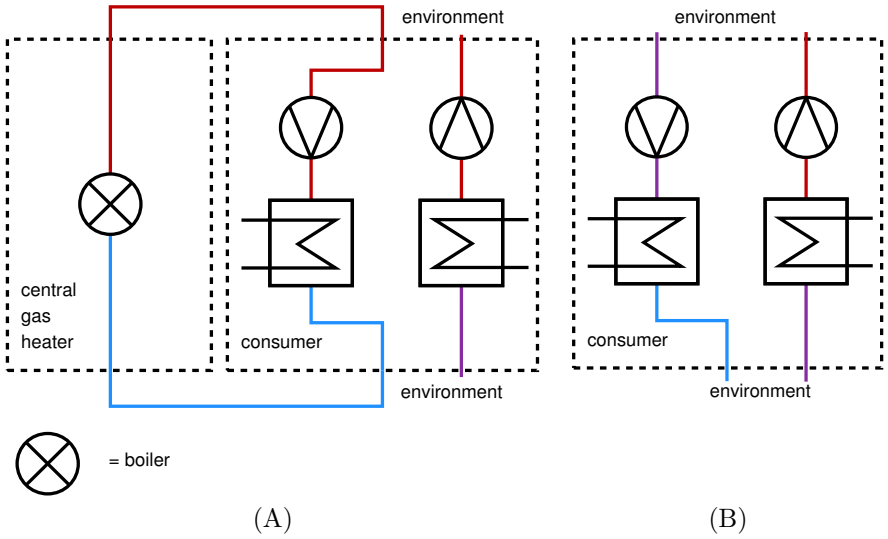

Figure 13: (A): district heating and stand-alone cooling schematic, (B): stand-alone schematic

the San Francisco Bay, which has relatively constant temperatures between 10 °C and 19 °C. This temperature range is a level at which both heat pumps and chillers can operate with high efficiency. The water heat exchanger in the Cologne case exchanges heat with the Rhine, whose temperature ranges from 6 °C in winter to 24 °C in summer. Together with the fact that high heat demands occur only during winter and high cold demands during summer in Cologne, this leads to a large improvement potential through the inclusion of other heat and cold sources such as solar thermal panels and seasonal heat and cold storage.

Fig. 14 (C) and Fig. 14 (D) show the normalized relative CO_2 emissions for the San Francisco case and Cologne case respectively, with the emission factors as in Tab. 2, taken from [4], [54] and [18]. Compared to the primary energy results, the CO_2 results show a much smaller gap between the district heating and the stand-alone case for San Francisco. This is due to the relatively high electricity CO_2 emission factor. For Cologne, the difference in emission is much closer to the difference in primary energy. For San Francisco, a reduction of 18% from district heating to the stand-alone solution could be achieved. For Cologne, this value is 47%. As options (2) to (5) are all electric systems the relative changes are proportional for primary energy consumption, CO_2 emissions and energy costs.

Table 2: CO_2 emission factors used in simulation in $\frac{kg_{CO2,eq}}{kWh}$

Energy carrier	San Francisco	Cologne
Natural gas	0.181	0.250
Electricity	0.788	0.565

For both locations, the results show that bidirectional LTN offer potential for primary energy and CO_2 emission reductions, especially when used with multiple heat and cold sources and agent-based control in order to achieve beneficial network temperatures.

Fig. 14 (E) and Fig. 14 (F) show the normalized energy costs for both scenarios. Tab. 3 shows the energy costs that are used for the simulation, taken from [34], [7], [56] and [44].

Table 3: Energy prices used in simulation in $\frac{cent_{Euro/Dollar}}{kWh}$

Energy carrier	San Francisco	Cologne
Natural gas	5.08	5.80
Electricity	15.34	29.16

The San Francisco results show that technologies

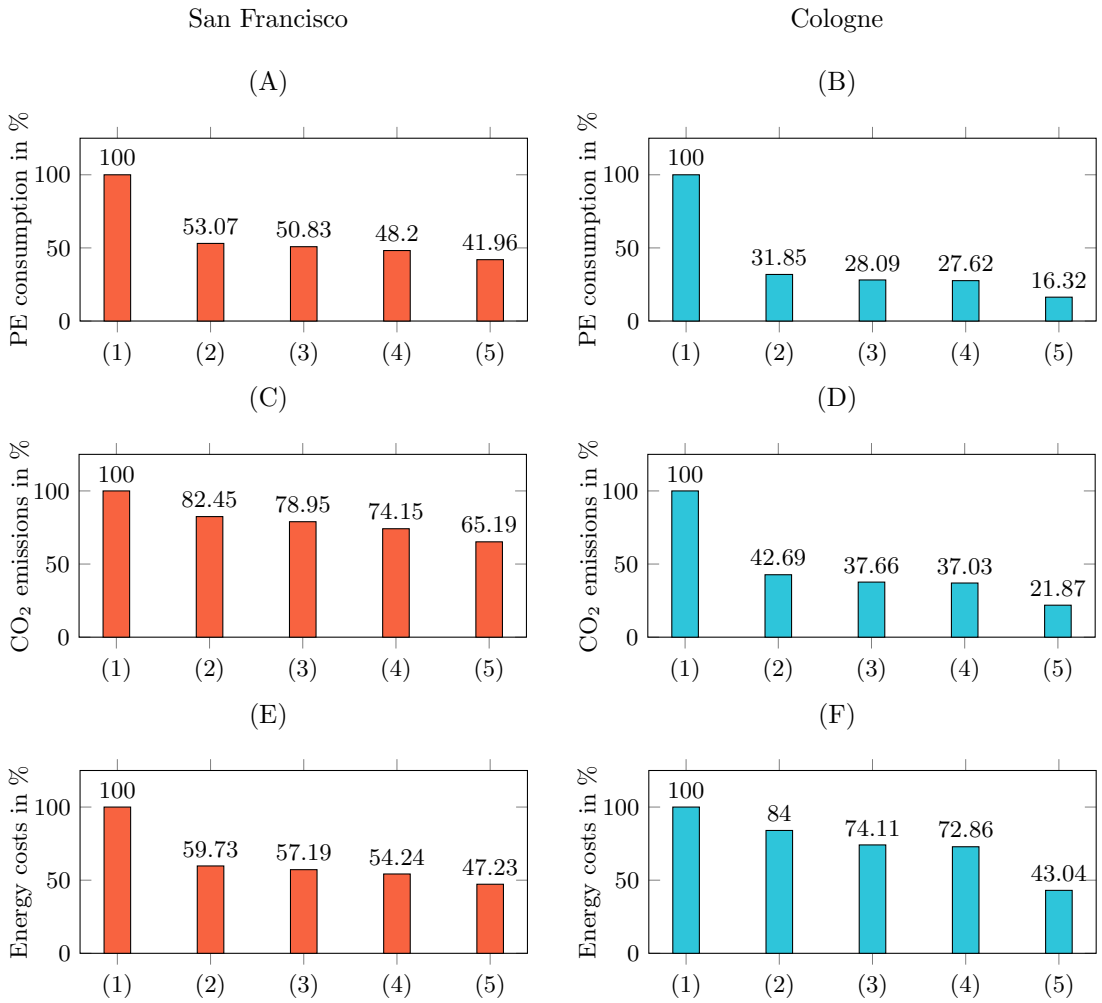

Figure 14: **Case study results:** (A) and (B) normalized primary energy consumption, (C) and (D) normalized CO_2 emissions, (E) and (F) normalized cost of operation
Scenarios: (1) District heating with stand-alone cooling, (2) stand-alone heating and cooling, (3) unidirectional LTN with free-floating temperature, (4) bidirectional LTN with free-floating temperature, (5) bidirectional LTN with agent-based control

using mainly electricity for heat generation are much more cost effective than gas-fired district heating without cogeneration. By using stand-alone heat pumps instead of district heating, the energy costs can be reduced by 40% because the price for electricity is low in California. The best scenario with a bidirectional LTN and agent-based control offers a total reduction of 53%. For Cologne, the difference in energy costs between district heating and the stand-alone solution is much lower due to the significantly higher electricity prices in Germany. However, the best technology with a bidirectional LTN with agent-based control achieves a reduction of 57% compared to the district heating case. The savings of 53% and 57% are in good agreement with [32], who describes a 62% reduction of operating cost for the LTN in Chur compared to the previously installed heating and cooling system.

For a complete economic evaluation, the net present value analysis of the competing technologies needs to be made. For this analysis, the investment costs need to be known. However, in the case of bidirectional LTN these investments are only known by a limited number of people as there are only a few demonstration projects available so far. Furthermore, other economic benefits, such as maintenance and usage of roof and floor space should be considered.

The results should be viewed keeping in mind that one focus of this work is operation optimization of bidirectional LTN. However, the control of all evaluated technologies could be further developed. Such developments could lead to further reductions of primary energy consumption, emissions and energy costs in all cases. Using combined heat and power units or waste heat instead of gas-fired boilers in the district heating case would also lead to different results that would benefit the performance of the conventional district heating system. Another point of discussion is the selection of primary energy factors and emission factors. Such factors always carry an uncertainty. As these values are usually calculated using life cycle analysis, in which many assumptions are made, factors can vary depending on the party that conducted the analysis. A further aspect is the date of publication, which varies a lot in the case of primary energy factors. Also, due to the increased integration of renewables in the electricity grid, the primary energy factors are changing.

4.2 Performance of agent-based control

As the functionality of the control approach is independent of the chosen location, only the San Francisco results are discussed in the following in order to avoid redundancy.

Fig. 15 shows the average of the four temperature measurement points in the agent-based control approach in comparison to the optimized set point of 20 °C and the temperature trajectory in the case of a bidirectional network with free-floating temperature.

The figure shows that the system does not have enough heating capacity to keep the temperature at the optimal set point in winter. The control error is up to 3 K. This problem could be solved by implementing more solar thermal panels or other heat sources. This is, however, a question of design optimization and is out of scope of this paper. The agent-based control is able to keep the average system temperature within a margin of 2 K around the set point during times in which the heat and cold demand in the system is more balanced. The error of 2 K during summer only occurs when the solar thermal plant is activated, which indicates that it could be lowered by improving the control of the solar thermal plant. During most times, the control error is less than 1 K.

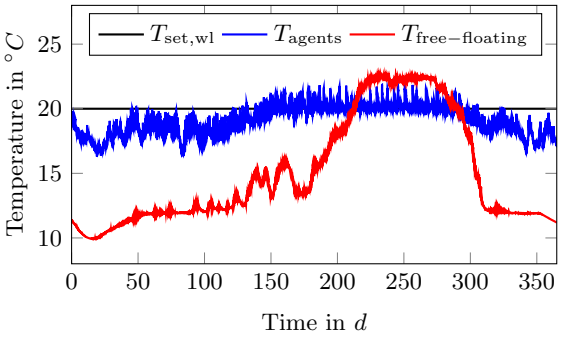

Figure 15: Average temperature trajectory with agent-based control and with free-floating temperatures for San Francisco

In general the agent-based control in combination with multiple sources keeps the network temperature much closer to the optimal set point than the free-floating approach, which leads to the improved performance presented above.

Fig. 16 shows the temperature in the warm line of the network at the four points of measurement. The temperatures vary widely and the assumption that a single temperature for each line is sufficient to describe the state of a bidirectional network is proven to be wrong. The temperatures T_1,T_3 and T_4 appear to be relatively stable whereas T_2 shows high frequency fluctuations of up to 9 K. Fig. 17 shows the mass flow rates at the points of temperature measurement. The highest mass flow rates and also the highest variation in mass flow rates are at the T_2 temperature measure-

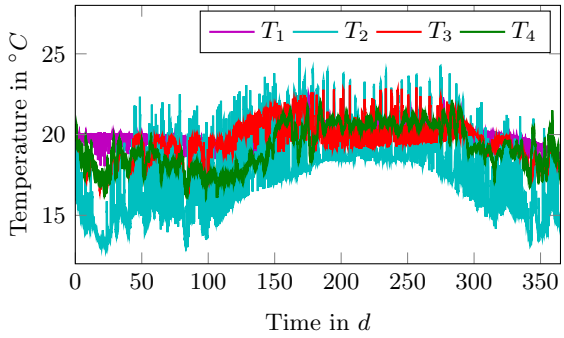

Figure 16: Temperature variation with agent-based control for San Francisco

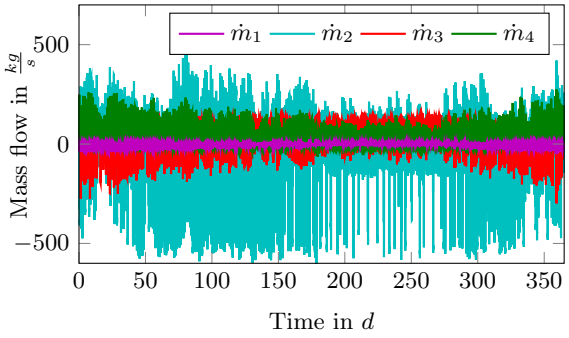

Figure 17: Mass flow variation with agent-based control for San Francisco

ment. This indicates that the point of measurement is a place where a large amount of fluid is bypassed between the warm and cold line, as large mass flows should mainly appear at bypass points in a network with reasonably well distributed heat and cold demands. A comparison to a mass flow rate measurement directly at the water heat exchanger and the fact that the water heat exchanger is used as the bypass whenever storage or solar thermal plants are not active support this observation.
The observed temperature variation does however not constitute a serious problem for the performance of the LTN. By comparing the bidirectional agent-based control case with the free-floating temperature approach and the optimization minimum (the case

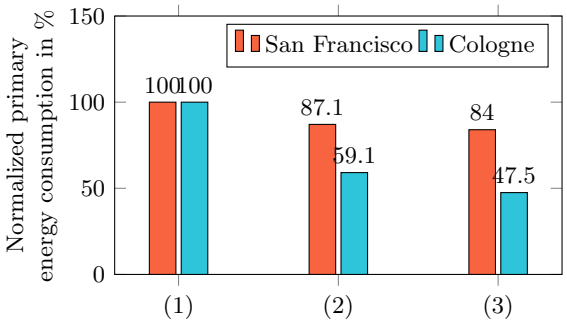

Figure 18: Agent-based control performance with (1) Free floating temperature (2) Bidirectional agent-based control (3) Optimization minimum

in which heat pumps are used with an ideal heat source at $T_{set,wl}$ and chillers with an ideal heat sink at $T_{set,cl} = T_{set,wl} - 4K$), it becomes clear that the agent-based approach achieved for San Francisco a 13% reduction at a maximum possible reduction of 16% (see Fig. 18). The remaining 3% could possibly be achieved by optimizing the design of the system, such as adding more heat sources. For Cologne, a reduction of 41% out of possible 56% was achieved.

5 Conclusion

Bidirectional LTN lead to an improvement in operation efficiency and can effectively be controlled with agent-based control, which aids the modular extension of such LTN systems. The agent-based control successfully coordinated various heat and cold sources to keep the network temperature around a specified set point. For both locations, the bidirectional LTN with agent-based control is the most efficient technology. In comparison to a conventional gas-fired district heating system, the optimized LTN leads to primary energy consumption reductions of 58% and 84% in the US and German scenario, respectively. Reductions of CO_2 emissions are 35% and 78%, and reductions of energy costs 53% and 57%. The savings are in good agreement with the results from existing demonstration projects. Another conclusion is that a constant set point for the pipe temperatures is sufficient for the analyzed systems.

6 Acknowledgements

This research was supported by the Assistant Secretary for Energy Efficiency and Renewable Energy, Office of Building Technologies of the U.S. Department of Energy, under Contract No. DE-AC02-05CH11231. This work was also funded by Lawrence Berkeley National Laboratory through the Laboratory Directed Research and Development (LDRD) Program

This work emerged from the Annex 60 project, an international project conducted under the umbrella of the International Energy Agency (IEA) within the Energy in Buildings and Communities (EBC) Programme. Annex 60 developed and demonstrated new generation computational tools for building and community energy systems based on Modelica, Functional Mockup Interface and BIM standards.

We gratefully acknowledge the financial support for Felix Bünning from the German Academic Exchange Service (DAAD) through its Thematic Network "ACalNet".

A Location parameters

Table 4: Parameters for the location San Francisco

Parameter	Value	Unit
A_{floor}	$170,000$	m^2
$\dot{Q}_{\text{nom}}$	$10,000$	kW
Q_h	$24.204E9$	kWh
Q_c	$10.348E9$	kWh

Table 5: Parameters for the location Cologne

Parameter	Value	Unit
A_{floor}	$170,000$	m^2
$\dot{Q}_{\text{nom}}$	$10,000$	kW
Q_h	$24.204E9$	kWh
Q_c	$10.348E9$	kWh

B Model parameters

Table 6: Parameters for bidirectional agent-based control LTN model of San Francisco

Parameter	Value	Unit
Heat pumps		
η_{c}	0.45	$-$
$\triangle T_{\mathrm{eva}}$	2	K
$\triangle T_{\mathrm{con}}$	2	K
$T_{\mathrm{sup,space}}$	30	°C
$T_{\mathrm{ret,space}}$	25	°C
$T_{\mathrm{sup,hotwat}}$	60	°C
Chiller		
η_{c}	0.45	-
$\triangle T_{\mathrm{eva}}$	2	K
$\triangle T_{\mathrm{con}}$	2	K
$T_{\mathrm{sup,space}}$	16	°C
$T_{\mathrm{ret,space}}$	20	°C
Network		
$\triangle T_{\mathrm{nominal}}$	4	K
$\dot{m}_{\mathrm{nominal}}$	$\frac{\dot{Q}_{\mathrm{nominal}}}{cp_{\mathrm{w}} \cdot \triangle T_{\mathrm{nominal}}}$	$\frac{kg}{s}$
v_{nominal}	1.5	$\frac{m}{s}$
Pipes		
l_{total}	8	km
R_{nominal}	100	$\frac{\mathrm{Pa}}{\mathrm{m}}$
d_{i}	71	cm
d_{ins}	20	cm
λ_{ins}	0.04	$\frac{\mathrm{W}}{\mathrm{mK}}$
PI controller		
P	$2.5E6$	$\frac{\mathrm{W}}{\mathrm{K}}$
T_{i}	1000	s
y_{max}	$1.2E7$	-
y_{min}	$-1.2E7$	-
Seasonal Storage		
V	$1.0E6$	m^3
Solar thermal plant		
A	$2.0E4$	m^2
Temperature set points		
$T_{\mathrm{set,wl}}$	20	°C
$T_{\mathrm{set,cl}}$	16	°C

Table 7: Deviating parameters for bidirectional agent-based control LTN model Cologne

Parameter	Value	Unit
Seasonal Storage		
V	$2.0E6$	m^3

Table 8: Parameters for district heating model

Parameter	Value	Unit
Central heat supplier		
T_{sup}	90	°C
T_{ret}	60	°C
η	0.95	$-$
Pipes		
l_{total}	8	km
R_{nominal}	100	$\frac{\mathrm{Pa}}{\mathrm{m}}$
d_{i}	26	cm
d_{ins}	40	cm
λ_{ins}	0.035	$\frac{\mathrm{W}}{\mathrm{mK}}$

References

[1] J. Ansari, A. Gholami, and A. Kazemi. Multi-agent systems for reactive power control in smart grids. *International Journal of Electrical Power & Energy Systems*, 83: 411–425, 2016.

[2] F. Bünning, R. Sangi, and D. Müller. A modelica library for the agent-based control of building energy systems. *Applied Energy*, 193: 52–59, 2017.

[3] J. Cai, D. Kim, R. Jaramillo, J. E. Braun, and J. Hu. A general multi-agent control approach for building energy system optimization. *Energy and Buildings*, 127:337 – 351, 2016. ISSN 0378-7788.

[4] M. Deru and P. Torcellini. Source energy and emission factors for energy use in buildings. Technical Report NREL/TP-550-38617, National Renewable Energy Laboratory, 2007.

[5] B. Di Pietra, F. Zanghirella, and G. Puglisi. An evaluation of distributed solar thermal "net metering" in small-scale district heating systems. *Energy Procedia*, 78:1859–1864, 2015.

[6] DIN Deutsches Institut für Normung e. V. DIN V 18599 2016, 2016.

[7] Electricity Local. California electricity rates & consumption. http://www.electricitylocal.com/states/california/, 2017. Accessed on: 03-03-2017.

[8] J. Fuetterer and A. Constantin. Energy concept for the e.on erc main building. *E.ON Energy Research Center Series*, 4, Issue 9, 2014.

[9] T. Gautschi. Anergienetze in Betrieb. Technical Report 66, Amstein + Walthert AG, 2015.

[10] Gemeinde Visp, CH. Anergienetz, eine erdölunabhängige Energieversorgung. Medienkonferenz, 2007.

[11] K. M. Heissler, L. Franke, I. Nemeth, and T. Auer. Modeling low temperature district heating networks for the utilization of local energy potentials. *Bauphysik*, 38(6):372–377, 2016.

[12] S. Henchoz, P. Chatelan, F. Maréchal, and D. Favrat. Key energy and technological aspects of three innovative concepts of district energy networks. *Energy*, 117(2):465–477, 2016.

[13] M. Huber, S. Brust, T. Schütz, A. Constantin, R. Streblow, and D. Müller. Purely agent based control of building energy supply systems. In *ECOS - International Conference on Efficiency, Cost, Optimization, Simulation and Environmental Impact of Energy Systems*, 2015.

[14] L. Hurtado, P. Nguyen, and W. Kling. Smart grid and smart building inter-operation using agent-based particle swarm optimization. *Sustainable Energy, Grids and Networks*, 2: 32–40, 2015.

[15] Z. Jiang. Agent-based control framework for distributed energy resources microgrids. In *IEEE/WIC/ACM International Conference on Intelligent Agent Technology*, 2006.

[16] Kanton St. Gallen. Amtsblatt Nr.7, M15, 2016.

[17] C.-S. Karavas, G. Kyriakarakos, K. G. Arvanitis, and G. Papadakis. A multi-agent decentralized energy management system based on distributed intelligence for the design and control of autonomous polygeneration microgrids. *Energy Conversion and Management*, 103:166–179, 2015.

[18] KEA Klimaschutz- und Energieagentur Baden-Wrttemberg GmbH. Co2-emissionsfaktoren. http://www.kea-bw.de/service/emissionsfaktoren/, 2016. Accessed on: 03-03-2017.

[19] M. R. B. Khan, R. Jidin, and J. Pasupuleti. Multi-agent based distributed control architecture for microgrid energy management

and optimization. *Energy Conversion and Management*, 112:288–307, 2016.

[20] K. Kok, B. Roossien, P. MacDougall, O. van Pruissen, G. Venekamp, R. Kamphuis, J. Laarakkers, and C. Warmer. Dynamic pricing by scalable energy management systemsfield experiences and simulation results using powermatcher. In *Power and Energy Society General Meeting, 2012 IEEE*, pages 1–8. IEEE, 2012.

[21] P. Kräuchi and M. Kolb. Simulation thermischer arealvernetzung mit ida-ice. In *Fourth German-Austrian IBPSA Conference - Berlin University of the Arts*, pages 205–211, 2012.

[22] P. Kräuchi and M. Kolb. Modellbildung für thermische Arealvernetzung mit IDA-ICE. In *Fifth German-Austrian IBPSA Conference - RWTH Aachen University*, pages 160–165, 2014.

[23] P. Kräuchi, T. Schluck, and M. Sulzer. Modelling of low temperature heating networks with IDA-ICE. In *Proceedings of International Conference CISBAT 2015 Future Buildings and Districts Sustainability from Nano to Urban Scale*, number EPFL-CONF-213420, pages 827–832. LESO-PB, EPFL, 2015.

[24] T. Kusuda and P. R. Achenbach. Earth temperature and thermal diffusivity at selected stations in the united states. Technical report, DTIC Document, 1965.

[25] E. Kuznetsova, Y.-F. Li, C. Ruiz, and E. Zio. An integrated framework of agent-based modelling and robust optimization for microgrid energy management. *Applied Energy*, 129:70–88, 2014.

[26] Landesamt für Natur, Umwelt und Verbraucherschutz - Nordrhein-Westfalen. Wassertemperatur der Station D.-Flehe im Jahr 2015. http://luadb.lds.nrw.de/LUA/hygon/pegel.php?stationsname_t=D.-Flehe&yAchse=Standard&hoehe=468&breite=724&jahr=2015&jahreswerte=ok&nachSuche=&meifocus=&neuname=, 2016. Accessed on: 11-10-2016.

[27] Lauber IWISA AG. Eine erdölunabhängige Energieversorgung. Technical report, 2012.

[28] Lennar. The San Francisco Shipyard. https://www.lennar.com/new-homes/california/san-francisco-bay-area/san-francisco/the-san-francisco-shipyard, 2016. Accessed: 11-10-2016.

[29] H. Li and S. J. Wang. Challenges in smart low-temperature district heating development. *Energy Procedia*, 61:1472–1475, 2014.

[30] H. Lund, S. Werner, R. Wiltshire, S. Svendsen, J. E. Thorsen, F. Hvelplund, and B. V. Mathiesen. 4th generation district heating (4gdh): Integrating smart thermal grids into future sustainable energy systems. *Energy*, 68: 1–11, 2014.

[31] D. Müller, M. R. Lauster, A. Constantin, M. Fuchs, and P. Remmen. AixLib - An Open-Source Modelica Library within the IEA-EBC Annex 60 Framework. In *BauSIM - Dresden*, 2016.

[32] M. Nani. Anergienetze und Wärmepumpen, HOVAL. http://www.fws.ch/tl_files/download_d/Downloads/FWS-Tagung%202014/Marco-Nani-Anergienetze.pdf, 2014. Accessed on: 05-06-2017.

[33] U. of Wisconsin-Madison. Solar Energy Laboratory and S. A. Klein. *TRNSYS, a transient system simulation program*. Solar Energy Laborataory, University of Wisconsin–Madison, 1979.

[34] Pacific Gas and Electric Company. Residential average gas rate, february 2017 forecast, 2017.

[35] A. Prasanna, N. Vetterli, V. Dorer, and M. Sulzer. Modelling the suurstoffi district based on monitored data to analyse future

scenarios for energy self-sufficiency. In *19. Status-Seminar Forschen für den Bau im Kontext von Energie und Umwelt*, 2016.

[36] B. M. Radhakrishnan and D. Srinivasan. A multi-agent based distributed energy management scheme for smart grid applications. *Energy*, 103:192–204, 2016.

[37] M. Rahman, M. Mahmud, A. Oo, H. Pota, and M. Hossain. Agent-based reactive power management of power distribution networks with distributed energy generation. *Energy Conversion and Management*, 120:120–134, 2016.

[38] P. Remmen, M. Lauster, M. Mans, M. Fuchs, T. Osterhage, and D. Müller. Teaser: an open tool for urban energy modelling of building stocks. *Journal of Building Performance Simulation*, pages 1–15, 2017.

[39] RVG Rheinauhafen Verwaltungsgesellschaft mbH. Die Eckdaten des Rheinauhafens. http://www.rheinauhafen-koeln.de/Uebersicht, 2016. Accessed on: 11-10-2016.

[40] T. Schluck, P. Kräuchi, and M. Sulzer. Non-linear thermal networks - how can a meshed network improve energy efficiency? In *Proceedings of International Conference CISBAT 2015 Future Buildings and Districts Sustainability from Nano to Urban Scale*, number EPFL-CONF-213421, pages 779–784. LESO-PB, EPFL, 2015.

[41] P. H. Shaikh, N. B. M. Nor, P. Nallagownden, I. Elamvazuthi, and T. Ibrahim. Intelligent multi-objective control and management for smart energy efficient buildings. *International Journal of Electrical Power & Energy Systems*, 74:403–409, 2016.

[42] S. Skarvelis-Kazakos, P. Papadopoulos, I. G. Unda, T. Gorman, A. Belaidi, and S. Zigan. Multiple energy carrier optimisation with intelligent agents. *Applied Energy*, 167:323–335, 2015.

[43] STROBEL-VERLAG GmbH & Co. KG . Dämmstandards von Fernwärmeleitungen. In *IKZ-Haustechnik*, volume 8, 2014.

[44] Strompreise.de. Strompreis pro kilowattstunde. https://www.strompreise.de/strompreis-kwh/, 2017. Accessed on: 03-03-2017.

[45] R. Stulz, S. Tanner, R. Sigg, and F. Sioshansi. Swiss 2000-watt society: A sustainable energy vision for the future. *Energy, Sustainability and the Environment. Oxford, UK: Elsevier Inc*, pages 477–496, 2011.

[46] M. Sulzer. Effizienzsteigerung mit Anergienetzen: Potentiale – Konzepte – Beispiele. Technical report, INRETIS - Energie und Gebäudetechnik, 2011.

[47] M. Sulzer. Solarenergie und Anergienetze - sinnvoll oder unsinnig? - Grundlagen, Konzepte und Beispiele, 2013.

[48] M. Sulzer and T. Gautschi. ETH Zürich, Hönggerberg Masterplan Energie. In *15. Schweizerisches Status-Seminar "Energie- und Umweltforschung im Bauwesen"*, pages 431–443, 2008.

[49] M. Sulzer and D. Hangartner. Kalte Fernwärme (Anergienetze) - Grundlagen-/Thesenpapier. Technical report, Lucerne University of Applied Sciences and Arts, 2014.

[50] M. Sulzer, U. Menti, and R. Spörri. Maschen und knoten. *TEC21*, 34/2015:31–33, 2015.

[51] S. Summermatter and M. Sulzer. Solare Fernwärme im alpinen Raum – Wirtschaftlichkeitsanalyse. In *19. Status-Seminar Forschen für den Bau im Kontext von Energie und Umwelt*, 2016.

[52] The European Comission. Fifth generation, low temperature, high exergy district heating and cooling networks. http://cordis.europa.eu/project/rcn/194622_en.html, 2015. Accessed on: 26-09-2017.

[53] U.S. Department of Energy. Commercial reference buildings. http://en.openei.org/datasets/files/961/pub/, 2016. Accessed on: 11-10-2016.

[54] US Environmental Protection Agency. Emission Factors for Greenhouse Gas Inventories. https://www.epa.gov/sites/production/files/2015-07/documents/emission-factors_2014.pdf, 2014. Accessed on: 06-05-2017.

[55] U.S. National Oceanic and Atmosphere Administration. Water temperature table of all coastal regions. http://www.nodc.noaa.gov/dsdt/cwtg/all_meanT.html, 2016. Accessed on: 11-10-2016.

[56] Verivox. Verivox-verbraucherpreisindex gas. http://www.verivox.de/verbraucherpreisindex-gas/, 2017. Accessed on: 03-03-2017.

[57] N. Vetterli and M. Sulzer. Dynamic analysis of the low-temperature district network "suurstoffi" through monitoring. In *Proceedings of International Conference CISBAT 2015 Future Buildings and Districts Sustainability from Nano to Urban Scale*, number EPFL-CONF-213373, pages 517–522. LESO-PB, EPFL, 2015.

[58] M. Wetter. Modelica library for building heating; ventilation and air-conditioning systems. In *Proceedings of the 7th International Modelica Conference; Como; Italy; 20-22 September 2009*, number 43, pages 393–402. Linkping University Electronic Press; Linkpings universitet, 2009.

[59] M. Wetter. Co-simulation of building energy and control systems with the building controls virtual test bed. *Journal of Building Performance Simulation*, 4(3):185–203, 2011.

[60] M. Wetter, W. Zuo, T. S. Nouidui, and X. Pang. Modelica buildings library. *Journal of Building Performance Simulation*, 7(4): 253–270, 2014.

[61] E. Xydas, C. Marmaras, and L. M. Cipcigan. A multi-agent based scheduling algorithm for adaptive electric vehicles charging. *Applied Energy*, 177:354–365, 2016.

[62] D. Ye, M. Zhang, and D. Sutanto. Decentralised dispatch of distributed energy resources in smart grids via multi-agent coalition formation. *Journal of Parallel and Distributed Computing*, 83:30–43, 2015.

[63] F. Zach. Anergienetze - Optimierte Nutzung lokaler erneuerbarer Energieträger in urbanen Neubaugebieten – Beispiel Nordwestbahnhofe. Austrian Energy Agency, 2016.

[64] R. Zarin Pass, M. Wetter, and M. Piette. A thermodynamic analysis of a novel bidirectional district heating and cooling network. *In review*, 2017.